18th Brazilian Congress of Thermal Sciences and Engineering
November 16-20, 2020 (Online)

ENC-2020-0233
APPLICATION OF GLIMM SCHEME FOR DESCRIBING FLOW THROUGH POROUS MEDIA WITH KINEMATICAL CONSTRAINED FLUID FRACTION

Daniel Cunha da Silva
Maria Laura Martins-Costa
Laboratory of Theoretical and Applied Mechanics (LMTA) Mechanical Engineering Graduate Program (TEM-PGMEC), Universidede Federal Fluminense, Rua Passo da Pátria, 156, 24210-240, Niterói, RJ, Brazil
maria_laura@id.uff.br, danielcunha@id.uff.br

Rogério M. Saldanha da Gama
Mechanical Engineering Graduate Program (FEN), Universidade do Estado do Rio de Janeiro, Rua São Francisco Xavier, 524, 20550-013, Rio de Janeiro, Brazil
rsgama@terra.com.br

Abstract. *This work uses a constitutive relationship to describe the transition unsaturated-saturated and vice-versa, employing a Mixture Theory approach that ensures the hyperbolicity of the associated mathematical system. This relationship is continuous and differentiable, and its first derivative is an increasing positive function so that the amount of fluid that may exceed the porosity is controllable. This work presents a new variation of the Glimm scheme, with a strong trend to preserve symmetries, giving rise to computational solutions with reliable positions of rarefaction, shock, and contact shock waves. Comparisons with the classical Glimm method for problems with exact solutions show this important feature.*

Keywords: *Glimm Scheme, flow through porous media, transition saturated-unsaturated, Mixture Theory.*

1. INTRODUCTION

This work employs a very convenient constitutive relationship (Martins-Costa et al., 2019) to describe filling a porous media by a fluid, considering an approach of the Continuum Theory of Mixtures. In a Mixture Theory approach, the mixture consists of superposed continuous constituents that simultaneously occupy the whole mixture volume (Atkin and Craine, 1976; Rajagopal and Tao, 1995). The unsaturated porous matrix is considered a three-constituents mixture composed of one solid constituent (porous matrix), one liquid constituent (fluid), and a gas constituent – assumed a very low-density gas, included to account for the mixture compressibility.

This constitutive relationship guarantees that the system's hyperbolicity is maintained even when saturation is reached, as in Martins-Costa et al. (2017). Still, it also consists of a continuous and differentiable its first derivative being an increasing positive function. This important feature allows controlling the amount of fluid fraction that can exceed porosity. Besides, the constitutive relation used for the pressure allows obtaining the associated Riemann problems' solutions in a relatively simple way, since it provides explicit forms for the Riemann invariants.

The relevance of the system remaining hyperbolic is the possibility of using an appropriate methodology to simulate hyperbolic systems, such as the Glimm method.

This work presents a new variation of the Glimm method (1965), according to the Chorin methodology (1976), which guarantees solutions with more reliable rarefaction, shock, and contact shock wave positions, keeping low computational cost. Also, the new variation of the Glimm method has a strong tendency to preserve symmetries.

2. MECHANICAL MODEL

This work studies the isothermal flow of a Newtonian liquid through a porous matrix. The mechanical model consists of a mixture of three chemically non-reactive constituents: a slightly deformable solid constituent composing the porous matrix, a fluid constituent given by the Newtonian liquid, and a gaseous constituent with negligible inertia. It is not necessary to consider neither the solid constituent's behavior (assumed slightly deformable) nor the gaseous component (a very rarefied gas, included only to consider the compressibility of the mixture). Under these hypotheses, to study the flow of the fluid constituent through the porous matrix, it suffices to solve equations of mass and linear momentum conservation for the fluid constituent, given by

$$\begin{aligned}&\frac{\partial \rho_F}{\partial t}+\operatorname{div}\left(\rho_F \mathbf{v}_F\right)=0\\&\rho_F\left[\frac{\partial \mathbf{v}_F}{\partial t}+\left(\nabla \mathbf{v}_F\right)\mathbf{v}_F\right]=\operatorname{div}\mathbf{T}_F+\rho_F\mathbf{b}_F+\mathbf{m}_F\end{aligned} \tag{1}$$

where ρ_F is the fluid constituent mass density (local ratio between fluid constituent mass and mixture volume) $\mathbf{v}_F$ its velocity in the mixture, $\mathbf{T}_F$ is the partial stress tensor, $\mathbf{b}_F$ is the fluid constituent body force and $\mathbf{m}_F$ is the momentum supply acting on the fluid constituent due to its interaction with the remaining constituents of the mixture. The momentum supply is zero for the mixture: $\sum_{i=1}^{N}\mathbf{m}_F=0$.

At this point, the fluid fraction, actually the ratio between the fluid constituent mass density ρ_F and the fluid mass density ρ_f (under a Continuum Mechanics viewpoint) is defined as $\phi=\rho_F/\rho_f$ and the porous matrix porosity is defined as ε. When $\phi=\varepsilon$ the porous matrix is saturated.

Neglecting the Darcian term (Srinivasan and Rajagopal, 2014) – a reasonable hypothesis for highly permeable porous media and/or minimal viscosity fluids, the momentum supply to the fluid constituent is given by

$$\mathbf{m}_F=-\frac{\mu_f D}{K}\nabla\phi \tag{2}$$

where μ_f is the fluid viscosity and K represents the specific permeability of the porous matrix (both in a Continuum Mechanics approach), and D is a diffusion coefficient.

The partial stress tensor is analogous to Cauchy tensor in Continuum Mechanics. It is worth noting that if it is assumed symmetrical, the angular momentum balance is automatically satisfied. $\mathbf{T}_F$ is assumed to be proportional to the pressure acting on the fluid constituent and to the gradient of fluid constituent velocity (Williams, 1978). Also, the dominance of normal fluid stresses proposed by Allen (1986) is assumed, leading to the following relation

$$\mathbf{T}_F=-\phi p\,\mathbf{I} \tag{3}$$

where $p=p(\phi)$ is a pressure (assumed constant while the flow is unsaturated) and $\mathbf{I}$ is the identity tensor.

Now assuming all the quantities to depend solely on time t and on position x and the only nonvanishing component of the fluid constituent velocity, $\mathbf{v}_F$, is denoted by v. Defining a pressure $\bar{p}=\hat{p}(\phi)$ such that

$$\bar{p}=\frac{1}{\phi_f}\left(p+\frac{\mu_f D}{K}\right) \tag{4}$$

and assuming that body forces can be neglected, Eqs. (1)-(4) give rise to the following system:

$$\begin{aligned}&\frac{\partial}{\partial t}\phi+\frac{\partial}{\partial x}\left(\phi v\right)=0\\&\frac{\partial}{\partial t}\left(\phi v\right)+\frac{\partial}{\partial x}\left(\phi v^2+\bar{p}\right)=0\end{aligned} \tag{5}$$

In this work the following constitutive relation is employed (Martins-Costa et al., 2019)

$$\bar{p}=c_1^2\phi+c_2^2\frac{\phi}{\bar{\varepsilon}-\phi}-2c_1c_2\sqrt{\bar{\varepsilon}}\,\ln\left(\frac{\bar{\varepsilon}-\phi}{\bar{\varepsilon}}\right) \tag{6}$$

where c_1 and c_2 are positive real constants and $\bar{\varepsilon}=\varepsilon+\delta$, with $0<\delta<<1$, with the real number δ representing a limit, the fluid fraction may exceed the porosity ε. The inequality $\varepsilon\le\phi<\bar{\varepsilon}=\varepsilon+\delta$ characterizes supersaturation. It is important to note that when $\phi>\varepsilon$, any increase in the fluid fraction causes both the propagation speeds and the

pressures to experience fast growth. This allows the preservation of the hyperbolic nature of the partial differential equations system, providing a reasonable answer to the problem.

3. ASSOCIATE RIEMANN PROBLEM

The following initial value problem is the Riemann problem associated to (5)-(6)

$$\begin{aligned} &\frac{\partial}{\partial t}\phi+\frac{\partial}{\partial x}\left(\phi v\right)=0 \\ &\frac{\partial}{\partial t}\left(\phi v\right)+\frac{\partial}{\partial x}\left(\phi v^2+\overline{p}\right)=0 \end{aligned} \qquad \text{initial condition:} \quad \left(\phi,v\right)=\begin{cases}\left(\phi_L,v_L\right) & \text{if} \quad -\infty<x<0\\ \left(\phi_R,v_R\right) & \text{if} \quad 0<x<+\infty\end{cases} \tag{7}$$

where ϕ_L, ϕ_R, v_L and v_R are constants and $\overline{p}=\hat{p}\left(\phi\right)$ is given by Eq. (6).
Using as similarity variable $\xi=x/t$, the following Riemann problem associated to (5)-(6) is defined

$$\begin{bmatrix} -\frac{x}{t} & 1 \\ \overline{p}'-v^2 & -\frac{x}{t}+2v \end{bmatrix}\frac{d}{d\xi}\begin{bmatrix}\phi\\ \phi v\end{bmatrix}=\begin{bmatrix}0\\0\end{bmatrix} \qquad \text{with} \quad \left(\phi,v\right)=\begin{cases}\left(\phi_L,v_L\right) & \text{if} \quad \xi=x/t\to-\infty\\ \left(\phi_R,v_R\right) & \text{if} \quad \xi=x/t\to+\infty\end{cases} \tag{8}$$

where $\overline{p}'$ is the (always positive) first derivative of $\overline{p}$ with respect to ϕ, so that $\overline{p}$ is an increasing function of ϕ.

4. GLIMM METHOD

The complete solution of the associated Riemann Problem is presented in Martins-Costa et al. (2019), and it is employed as input to Glimm method (Glimm, 1965; Chorin, 1976). This method marches in time using the solution of a certain predetermined number of Riemann problems to approximate nonlinear hyperbolic problems. Glimm method can deal with complex wave interactions involving discontinuities, such as shock waves and material interfaces, in addition to satisfactorily showing smooth waves, such as rarefactions, in its solutions.

Although Glimm's scheme preserves the shock identity (shock magnitude and position) better than other numerical methodology such as a finite element method associated with a shock capture procedure, for instance, there is still a possibility of a certain possibility of an error in the position of the shock or rarefaction waves at any time. In the present work, a new variation of the Glimm method was developed to attenuate this error in the position of the waves (shock, contact shock and rarefaction), promoting a symmetric solution to the Riemann problems that have a symmetric solution.

Glimm's semi-analytical scheme is applied to the initial value problem associated with a one-dimensional non-linear hyperbolic system in the form of a conservation law.

$$\begin{aligned} &\frac{\partial}{\partial t}\left(\mathbf{u}\right)+\frac{\partial}{\partial x}\left(\mathbf{f}\left(\mathbf{u}\right)\right)=0 \\ &\mathbf{u}\left(x,0\right)=\mathbf{u}^0\left(x\right) \end{aligned} \qquad -L\le x\le L \quad \text{with } L\in\mathbb{R}^+ \text{ and } t\ge 0 \tag{9}$$

where $\mathbf{u}$ is such that $\mathbf{u}=\left(\phi,\phi v\right)^T$ with $i=1,\cdots,n$ and $\mathbf{f}\left(\mathbf{u}\right)$ is the flow function

The spatial domain $\left[-L,L\right]$ is discretized into $2M$ computing cells or finite volumes given by the real intervals $I_i=\left[x_{i-1/2},x_{i+1/2}\right]$ of size $\Delta x=x_{i+1/2}-x_{i-1/2}=L/M$, with $i=1,\cdots,2M$. For each spatial interval I_i, the location of its center x_i and its extremes $x_{i-1/2}, x_{i+1/2}$ are given respectively by

$$x_i=-L+\left(i-\frac{1}{2}\right)\Delta x \qquad x_{i-1/2}=x_i-\frac{\Delta x}{2} \qquad x_{i+1/2}=x_i+\frac{\Delta x}{2} \tag{10}$$

The initial condition $\mathbf{u}^0(x)$ is transformed into a constant function in each spatial interval I_i, in each interval I_i the initial condition assumes the status values equal to $\mathbf{u}_i^0 = \mathbf{u}^0(x_i)$, $i = 1, \cdots, 2M$, these values are updated at each step in time. The data at each time step $t = t_n$, $\mathbf{u}^n = \mathbf{u}(x, t_n)$, are also constant by parts, and the values for the spatial interval I_i are always constant and here denoted by $\mathbf{u}_i^n$. From these data the solution will evolve to a time $t_{n+1} = t_n + \Delta t$, $\Delta t > 0$.

The pairs $\mathbf{u}_{i-1}^n$, $\mathbf{u}_i^n$ and $\mathbf{u}_{i+1}^n$ define states on the left and right at the ends of the spatial interval I_i, $x_{i-1/2}$ and $x_{i+1/2}$ respectively, and consequently also define local Riemann problems centered on the same points. These Riemann problems have exact solutions, denoted by $\mathbf{u}_{i-1/2}^n(\xi)$ and $\mathbf{u}_{i+1/2}^n(\xi)$ respectively, where $\xi = x/t$ is the similarity variable.

The advance of the solution from time t_n to t_{n+1} in a spatial interval I_i occurs by the random choice of a state of the solutions $\mathbf{u}_{i-1/2}^n(\xi)$ and $\mathbf{u}_{i+1/2}^n(\xi)$ within the range I_i. The chosen state depends on a random or pseudo-random number θ in the range $(-1/2, +1/2)$.The solution is then updated as follows

$$\mathbf{u}_i^{n+1} = \begin{cases} \mathbf{u}_{i-1/2}^{n+1}\left(\theta \dfrac{\Delta x}{t}\right) & 0 \le \theta < \dfrac{1}{2} \\ \mathbf{u}_{i+1/2}^{n+1}\left(\theta \dfrac{\Delta x}{t}\right) & -\dfrac{1}{2} < \theta < 0 \end{cases} \tag{11}$$

The choice of the time interval Δt is determined by a Courant-Friedrichs-Lewy (CFL) condition, in such a way that no interaction between waves, shock, contact, or rarefaction, of the solutions $\mathbf{u}_{i-1/2}^n(\xi)$ and $\mathbf{u}_{i+1/2}^n(\xi)$ occurs within the spatial interval I_i. So, it comes that

$$\Delta t \le \frac{\frac{1}{2}\Delta x}{|\lambda|_{\max}} \tag{12}$$

where $|\lambda|_{\max}$ is the absolute value of the maximum shock propagation speed, considering all Riemann problems at a given time t_n.

The quality of the solution obtained by the Glimm method depends crucially on the random numbers $\{\theta_n\}$. A desirable statistical property of the number sequence $\{\theta_n\}$ is that it is evenly distributed over the interval $(-1/2, +1/2)$ (Olivier and Grönig, 1986). In the present work the sequence of random numbers $\{\theta_n\}$ is generated as follows

$$\theta_n = \hat{\theta}(n) = n\sqrt{\wp} - \left\lfloor n\sqrt{\wp} \right\rfloor - \frac{1}{2} \quad , \qquad n = 1, 2, \cdots \tag{13}$$

where $\wp$ is a prime natural number, and $\lfloor \bullet \rfloor$ is the largest integer function that can be defined as $\lfloor x \rfloor = \max\{m \in \mathbb{Z}, m < x\}$. In this work the sequence of random numbers $\{\theta_n\}$ is generated with $\wp = 5$.

Equation (10) states that in the Glimm method, the decision that is made depends on the sign of the random number θ. There is evidence that the momentary repetition of the θ sign causes errors in the positions of shock waves, contact shock and rarefaction waves, this evidence can be observed making the number always positive, for example.

In an attempt to mitigate this error in the wave positions, a methodology providing a Free Signal Randomness solution of the random number θ_n is proposed. It consists of the determination of two solutions by the Glimm method at each step in the time from t_n to t_{n+1}. One from the sequence $\{\theta_n\}$ presented before, and its restriction to the spatial interval I_i, denoted as $\left(\mathbf{u}_i^{n+1}\right)_+$ and given by

$$\left(\mathbf{u}_i^{n+1}\right)_+ = \begin{cases} \mathbf{u}_{i-1/2}^{n+1}\left(\theta_n \dfrac{\Delta x}{t}\right) & 0 \le \theta_n < \dfrac{1}{2} \\ \mathbf{u}_{i+1/2}^{n+1}\left(\theta_n \dfrac{\Delta x}{t}\right) & -\dfrac{1}{2} < \theta_n < 0 \end{cases} \tag{14}$$

The second solution is determined using the sequence $\{-\theta_n\}$, the symmetric additives of $\{\theta_n\}$, and their restriction to the spatial interval I_i denoted as $\left(\mathbf{u}_i^{n+1}\right)_-$ and given by

$$\left(\mathbf{u}_i^{n+1}\right)_- = \begin{cases} \mathbf{u}_{i-1/2}^{n+1}\left(-\theta_n \dfrac{\Delta x}{t}\right) & 0 \le -\theta_n < \dfrac{1}{2} \\ \mathbf{u}_{i+1/2}^{n+1}\left(-\theta_n \dfrac{\Delta x}{t}\right) & -\dfrac{1}{2} < -\theta_n < 0 \end{cases} \tag{15}$$

Finally, we obtain a solution independent of the sign of θ_n using the two solutions of the Riemann problems located at the ends of the interval I_i, $\mathbf{u}_{i-1/2}^n(\xi)$ and $\mathbf{u}_{i+1/2}^n(\xi)$, denoted by $\overline{\mathbf{u}}_i^n$ given by the arithmetic mean

$$\overline{\mathbf{u}}_i^{n+1} = \frac{\left(\mathbf{u}_i^{n+1}\right)_- + \left(\mathbf{u}_i^{n+1}\right)_+}{2} \tag{16}$$

5. RESULTS

In this section, the exact solutions of four examples of Riemann Problems related to the system are presented (7), which shows the four possibilities for solving the Riemann Problem. For these results, the parameters of the constitutive relationship (6) were considered $c_1 = c_2 = 1$ and a porosity $\varepsilon = 0.9$, with supersaturation of 2%, in other words, $\delta = 0.018$. Table 1 shows the initial conditions and the type of solution and the intermediate states of the four examples treated in this section; while, Table 2 shows the eigenvalues of the states on the left, the intermediate states and the states on the right and the shock speeds of the studied examples. It is worth noting that in the event of a shock wave, there is an inversion in the order of growth of the eigenvalues from the state on the left to the intermediate state and from the intermediate state to the state on the right.

Table 1. Left and right states, type of solution and intermediate states of fluid fraction and speed of the examples of Riemann problem solved for this section.

Riemann Problem	ϕ_L	v_L	ϕ_R	v_R	Solution	ϕ_*	v_*
I	0.7	-5.0	0.7	5.0	Rarefaction 1 - Rarefaction 2	0.117	0.000
II	0.7	5.0	0.7	-5.0	Shock 1 – Shock 2	0.908	0.000
III	0.8	0.0	0.5	0.0	Rarefaction 1 – Shock 2	0.668	1.144
IV	0.5	0.0	0.8	0.0	Shock 1 – Rarefaction 2	0.668	-1.144

Table 2. Eigenvalues and shock speeds of the studied examples.

Riemann Problem	λ_{1L}	s_1	λ_{1*}	λ_{2*}	s_2	λ_{2R}
I	-10.360	–	-2.195	2.195	–	10,360
II	-0.359	-16.850	-79.095	79.095	16.850	0,359
III	-8.993	–	-3.659	5.946	4.552	3,284
IV	-3.284	-4.552	-5.946	3.659	–	8.993

Two distinct partitions from the spatial range $-20 \le x \le 20$ are used, one with $\Delta x = 0.4$ and the other more refined with $\Delta x = 0.2$, to study the convergence and the particular features of the Glimm method. In both cases, the length Δt that determines the partition of the time interval was fixed with the value $\Delta t = 0.001$ for all simulations in this section. The CFL condition gives rise to

$$\left|\lambda\right|_{\max} = \frac{1}{2}\frac{\Delta x}{\Delta t} = \begin{cases} 100, & \Delta x = 0.2 \\ 200, & \Delta x = 0.4 \end{cases} \tag{17}$$

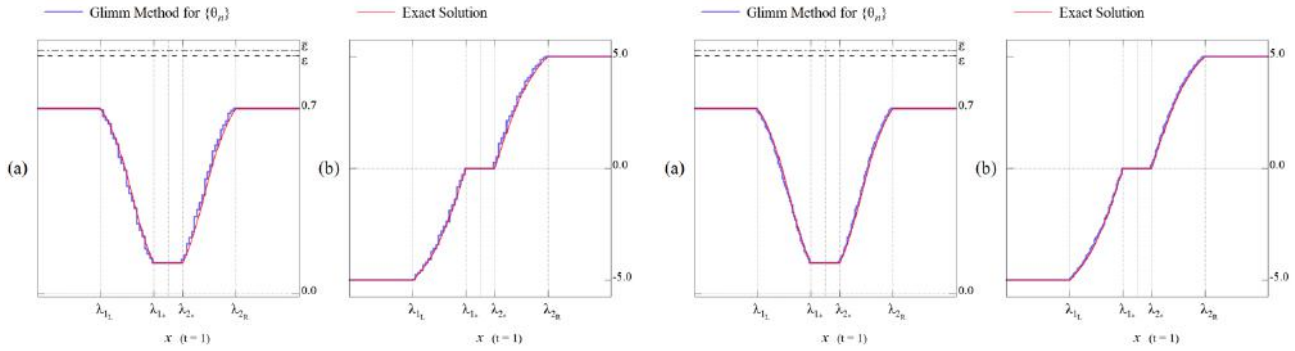

Figure 1. Graphical comparison between the exact solution of the Riemann Problem I and the solution obtained by the Glimm Method using $\{\theta_n\}$ for (a) fluid fraction and (b) velocity – left: $\Delta x = 0.4$; right: $\Delta x = 0.2$.

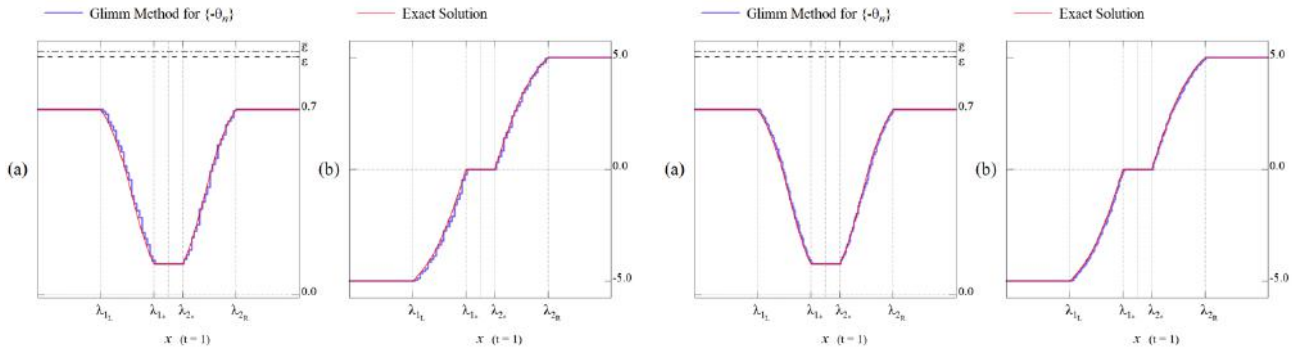

Figure 2. Graphical comparison between the exact solution of the Riemann Problem I and the solution obtained by the Glimm Method using $\{-\theta_n\}$ for (a) fluid fraction and (b) velocity – left: $\Delta x = 0.4$; right: $\Delta x = 0.2$.

In all the depicted results, the graphical comparison between the Glimm method's solutions and the exact solution of the Riemann problems is presented at time $t = 1$, which is when the similarity variable $\xi = x / t$ has the same numerical result of the spatial variable x.

Figures 1 to 3 depict the comparison between the exact solution of the problem I (described in Tab. 1) and its solution obtained by the Glimm method, considering Eqs. (13), (14), and (15), which correspond to the sequences $\{\theta_n\}$, $\{-\theta_n\}$ and the strategy proposed in this work that consists of arithmetic mean of the spatial interval, for $\Delta x = 0.4$ and $\Delta x = 0.2$. As expected, the new strategy presents better results than the sequences $\{\theta_n\}$and $\{-\theta_n\}$.

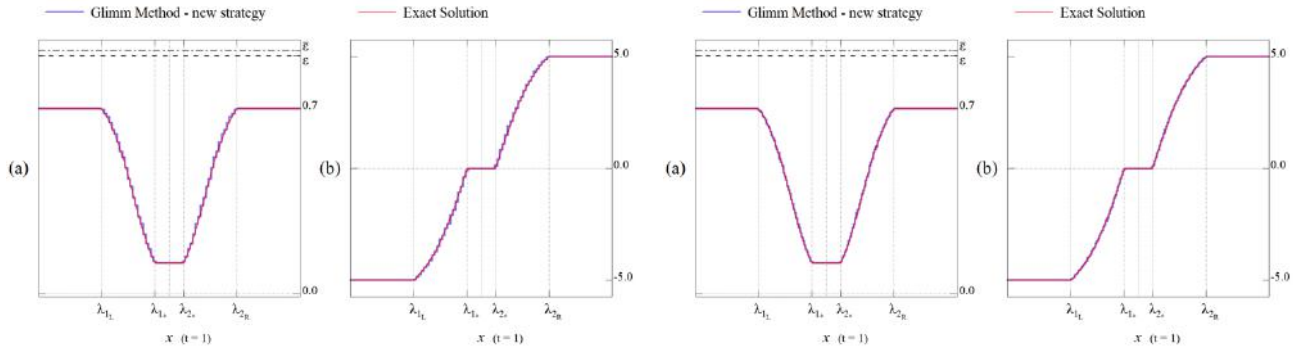

Figure 3. Graphical comparison between the exact solution of the Riemann Problem I and the solution obtained by the Glimm Method using the new strategy for (a) fluid fraction and (b) velocity – left: $\Delta x = 0.4$; right: $\Delta x = 0.2$.

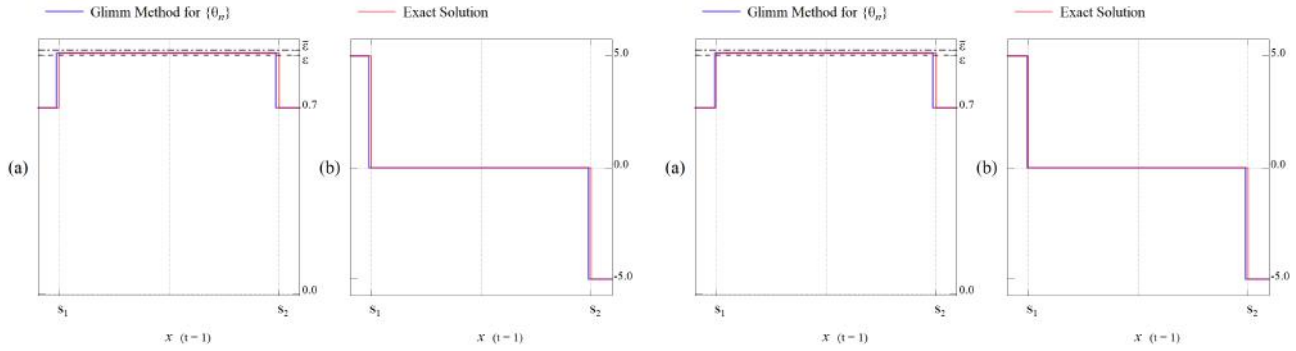

Figure 4. Graphical comparison between the exact solution of the Riemann Problem II and the solution obtained by the Glimm Method using $\{\theta_n\}$ for (a) fluid fraction and (b) velocity – left: $\Delta x = 0.4$; right: $\Delta x = 0.2$.

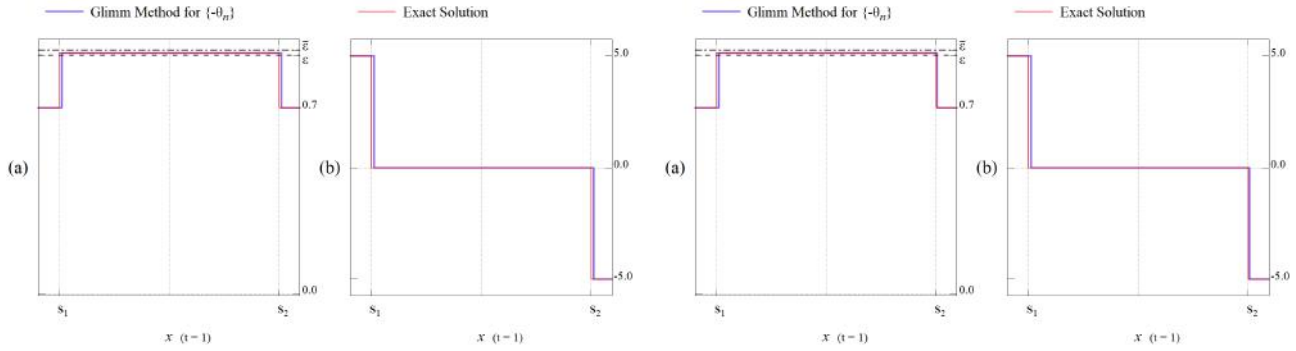

Figure 5. Graphical comparison between the exact solution of the Riemann Problem II and the solution obtained by the Glimm Method using $\{-\theta_n\}$ for (a) fluid fraction and (b) velocity – left: $\Delta x = 0.4$; right: $\Delta x = 0.2$.

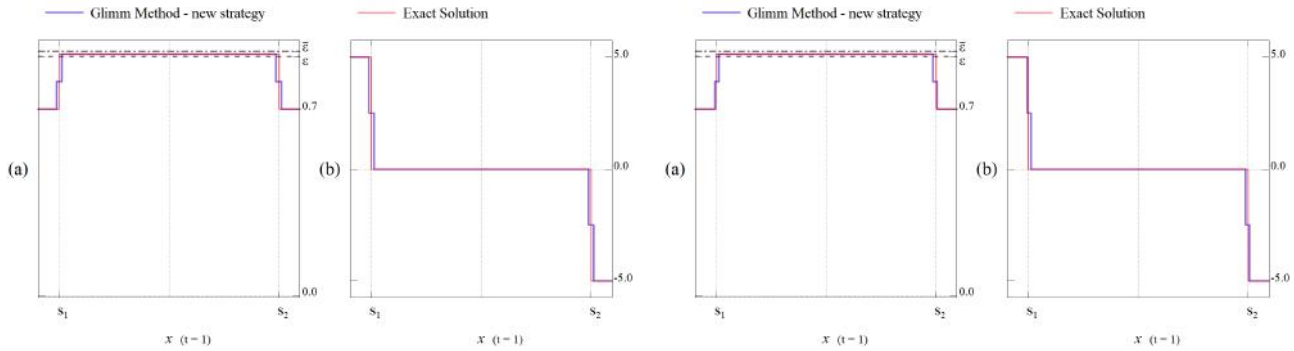

Figure 6. Graphical comparison between the exact solution of the Riemann Problem II and the solution obtained by the Glimm Method using the new strategy for (a) fluid fraction and (b) velocity – left: $\Delta x = 0.4$; right: $\Delta x = 0.2$.

Figures 4 to 6 compare the exact solution of the problem II (described in Tab. 1) with its solution obtained using the Glimm method, considering Eqs. (13), (14), and (15), which correspond to the sequences $\{\theta_n\}$, $\{-\theta_n\}$ and the strategy proposed in this work that consists of arithmetic mean of the spatial interval, for $\Delta x = 0.4$ and $\Delta x = 0.2$. As expected, the new strategy presents better results than the sequences $\{\theta_n\}$and $\{-\theta_n\}$. It is worth noting that in this case a very small supersaturation is allowed. The results related to the II present more adherence to the exact solution than those related to Problem I, probably due to the connection shock 1-shock 2

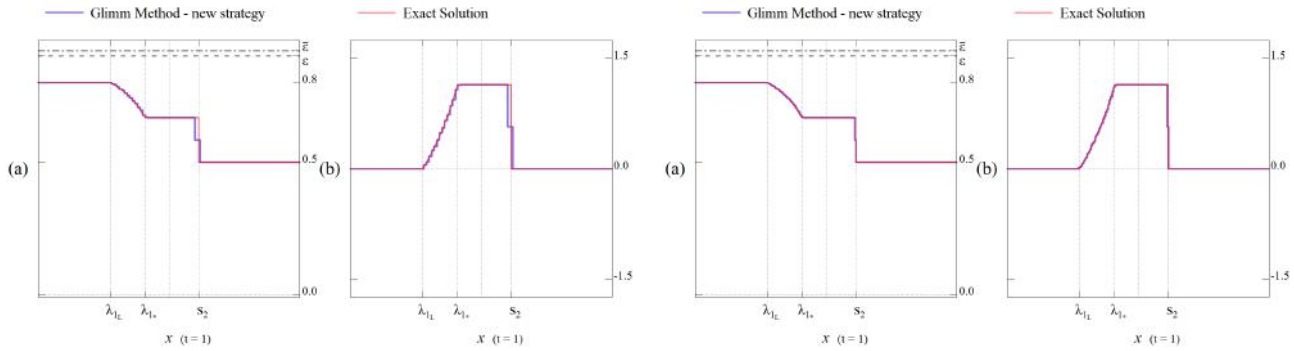

Figure 7. Graphical comparison between the exact solution of the Riemann Problem III and the solution obtained by the Glimm Method using the new strategy for (a) fluid fraction and (b) velocity – left: $\Delta x = 0.4$; right: $\Delta x = 0.2$.

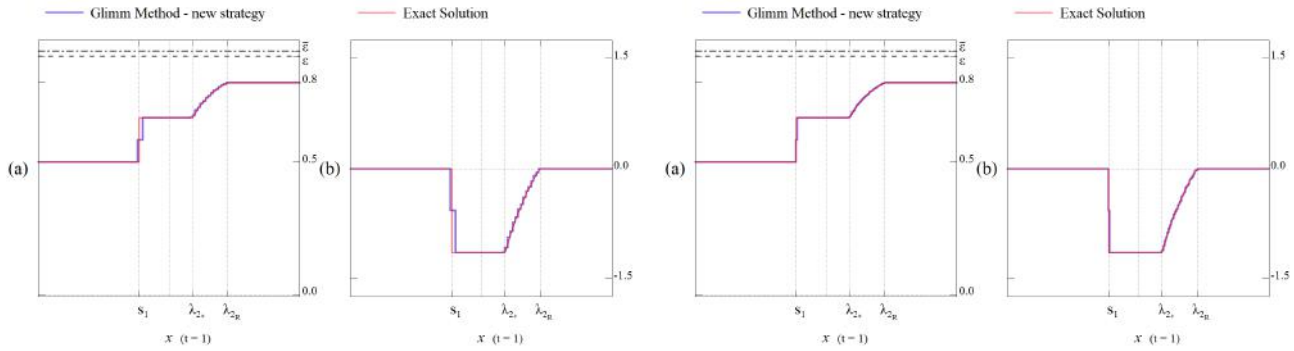

Figure 8. Graphical comparison between the exact solution of the Riemann Problem IV and the solution obtained by the Glimm Method using the new strategy for (a) fluid fraction and (b) velocity – left: $\Delta x = 0.4$; right: $\Delta x = 0.2$.

Finally, the comparison of the exact solution with its solution obtained using the Glimm method for Problems III and IV (described in Tab. 1) are depicted in Figs. 7 and 8, respectively. In these cases, only the strategy proposed in this work is shown.

6. FINAL REMARKS

A constitutive relation for the pressure allowing for a very small supersaturation was employed to preserve the hyperbolic nature of the mathematical system representing a flow through porous media allowing transitions unsaturated-saturated and vice-versa. The supersaturation is controlled, and whenever fluid fraction exceeds the porosity, any additional increase in the fluid fraction provokes a quick augmentation on the pressures and the propagation speeds.

The implementation of the Glimm method depends on the sign of the random number θ. A momentary repetition of the random number sign may cause errors in the positions of shock, rarefaction, and contact shock waves. This work proposed a methodology that is free from the signal randomness of the random number θ_n. It considers the sequences $\{\theta_n\}$and $\{-\theta_n\}$, making arithmetic mean of the spatial interval for distinct values of the spatial interval Δx. This new sequence presents better results than the original sequences, and the smaller the space interval, the better the results.

Anyway, it must be noticed that the fluid fraction has an upper bound that can be freely chosen, provided that it is higher than the porosity. It is also worth noticing that it is the first time that the Glimm scheme is employed in a problem with transition saturated/unsaturated and vice-versa.

7. ACKNOWLEDGEMENTS

The author D. Cunha da Silva acknowledges the financial support of Brazilian agency CAPES and the authors M.L Martins-Costa and R.M. Saldanha da Gama acknowledge the financial support of Brazilian agency CNPq.

8. REFERENCES

Allen, M. B., 1986. “Mechanics of multiphase fluid flows in variably saturated porous media”, *International Journal of Engineering Science*, Vol. 24, No. 3, pp. 339–351.

Atkin, R. J., Craine, R. E., 1976. “Continuum Theories of Mixtures. Basic theory and historical development”, *Quarterly Journal of Mechanics and Applied Mathematics*, Vol. 29, pp. 209-244.

Chorin, A.J. 1976. “Random choice solution of hyperbolic systems”. *Journal of Computational Physics*, Vol. 22, pp. 517–533.

Glimm, J, 1965. “Solutions in the large for nonlinear hyperbolic systems of equations”. *Communications on Pure and Applied Mathematics*, Vol. 18. pp. 697–715.

Olivier, H. and Grönig, H., 1986. “The random choice method applied to two-dimensional shock focusing and diffraction”, Journal of Computational Physics, Vol. 63, pp. 85–106.

Martins-Costa, M.L., Alegre, D.M., de Freitas Rachid, F.B., Jardim, L.G.C.M. and Saldanha da Gama, R.M., 2017. “A hyperbolic mathematical modeling for describing the transition saturated/unsaturated in a rigid porous medium”, *International Journal of Non-Linear Mechanics*, Vol. 95, pp. 168–177.

Martins-Costa, M.L., da Silva, D.C., da Silva, M.C. and Saldanha da Gama, R. M., 2019. “A New Constitutive Relation for Describing the Flow through Porous Media with Unsaturated–Saturated Transition”, *Mathematical Problems in Engineering*, Vol. 2019, Article ID 2347809, 12 pages https://doi.org/10.1155/2019/2347809.

Rajagopal, K. R. and Tao, L., 1995. *Mechanics of Mixtures*, Series on Advances in Mathematics for Applied Sciences Vol. 35, World Scientific, Singapore.

Smoller, J., 1983. *Shock-Waves and Reaction-Diffusion Equations*, Cambridge University Press, New York.

S. Srinivasan and K. Rajagopal, “A thermodynamic basis for the derivation of the Darcy, Forchheimer and Brinkman models for flows through porous media and their generalizations”, *International Journal of Non-Linear Mechanics*, Vol. 58, pp. 162– 166, 2014.

9. RESPONSIBILITY NOTICE

The authors are the only responsible for the printed material included in this paper.